Iran. J. Biotechnol. October 2022;20(4): e3136 DOI: 10.30498/ijb.2022.301092.3136

Research Article

MiR-582 Down-Regulates Lissencephaly-1 (*LIS1*) via P-Akt and MMP-2 to Inhibit Cholangiocarcinoma Cell Proliferation and Invasion

Guochao Liu, Tao Li, Lifeng Ma, Jianlong Wang, Zhaoqiang Yin*

Department of Minimally Invasive and Biliary Surgery, The Second Hospital of Hebei Medical University

*Corresponding author: Zhaoqiang Yin, Department of Minimally Invasive and Biliary Surgery, The Second Hospital of Hebei Medical University, No. 215 Heping West Road, Shijiazhuang, Hebei, 050000, China. Tel/ Fax: +86-31187046901, E-mail: yinzhaoqiang1981@hebmu.edu.cn

Background: Cholangiocarcinoma is a primary malignant tumor, and its progression involves oncogene activation, the absence of tumor suppressor gene, abnormal signaling pathways and miRNA expression. MiRNAs are abnormally expressed in many types of tumors.

Objective: This study aims to observe the effects of miR-582 on cholangiocarcinoma cell proliferation, S-phase arrest, migration and invasion and to analyze the regulation of miR-582 on *LIS1* to clarify the real role of miR-582 in cholangiocarcinoma development.

Materials and Methods: TCGA database of cholangiocarcinoma samples was analyzed. Dual fluorescence reporter and TargetScan were conducted to confirm whether *LIS1* was the target gene of miR-582. Effects of miR-582 and *LIS1* on HCC-9810 cell proliferation, S-phase cell ratio, migration and invasion were determined by CCK-8, Flow cytometry and Transwell, respectively, whereas the function of miR-582 on MMP-2 and P-Akt expression was identified by Western blotting. Nude mice xenograft model of cholangiocarcinoma was established to detect what miR-582 did for tumor growth.

Results:TCGA showed that miR-582 was lowly expressed and LIS1 was highly expressed in tumor tissues compared with adjacent tissues. MiR-582 targeted *LIS1* to inhibit MMP-2 and p-AKT expression. Transfection of miR-582 mimics could suppress HCC-9810 cell proliferation, S-stage arrest, migration and invasion, while *LIS1* worked oppositely. MiR-582 inhibitors promoted cell biological behavior, whereas *LIS1* siRNA was opposite. In nude mice xenograft model, miR-582 overexpression inhibited tumor growth.

Conclusions: It implies that miR-582 could negatively regulate *LIS1* to inhibit MMP-2 and P-Akt expression, thus suppressing cell invasion and proliferation in cholangiocarcinoma.

Keywords: Cholangiocarcinoma; *LIS1*; MMP-2; miR-582; p-AKT

1. Background

Cholangiocarcinoma or bile duct cancer, a rare tumor growing in the small tubes, accounts for 3% of all gastrointestinal tumors (1, 2). Its incidence and progression involve a complex regulatory mechanism including abnormal mRNA expression and changes of signaling pathways (3-5). Therefore, it is of great significance to find molecular targets for the early diagnosis and treatment of cholangiocarcinoma.

MicroRNAs(miRNA) are short, small, non-coding RNAs consisted of 21-25 nucleotides (6), which could regulate gene expression at post-transcriptional level. miRNAs can play a key biological role in life development (7), cell differentiation (8), apoptosis

Copyright *© 2022 The Author(s); Published by National Institute of Genetic Engineering and Biotechnology. This is an open access article, distributed under the terms of the Creative Commons Attribution-NonCommercial 4.0 International License (http://creativecommons.org/licenses /by-nc/4.0/) which permits others to copy and redistribute material just in noncommercial usages, provided the original work is properly cited.*

(9), lipid metabolism (10) and hormone secretion (11). Previous studies have confirmed abnormal miRNA expression, usually locating at tumor-related fragile sites in genomes, is likely involved in many types of tumors (12, 13). Studies indicate that miRNA expression in cholangiocarcinoma tissues largely differs from that in adjacent bile duct tissues, which includes miR-9, miR-302c, miR-199a-3p and miR-222 (14-17). Multiple studies reported that miR-582 was actively involved in hepatocellular carcinoma (18), cervical cancer (19) and osteosarcoma (20). However, the underlying mechanism of miR-582 in cholangiocarcinoma is rarely reported.

LIS1 gene, located at chromosome 17p13, participates in multiple protein interactions, and its expression level is related to many cell activities (21). Previous study suggests that retinoic acid could reduce the migration and invasion of human neuroblastoma cells by down-regulating *LIS1* expression (22). The regulatory role of *LIS1* in liver cancer (23), glioblastoma (24) and head and neck cancer (25) has also been reported, but its function in cholangiocarcinoma still needs to be explored.

2. Objective

Our study was set to observe the effects of miR-582 and its target gene *LIS1* on cholangiocarcinoma cellular proliferation, S-phase arrest, migration and invasion, thereby analyzing the working mechanism of miR-582 in cholangiocarcinoma.

3. Material and Methods

3.1. Sample Collection

71 pairs of cholangiocarcinoma and normal adjacent tissues were collected from April 2015 to July 2019 at the Second Hospital of Hebei Medical University (Hebei, China). All cases were staged according to the 2011 Union for International Cancer Control TNM classification of malignant tumors. Patients (41 males and 30 females; aged 43-76) did not receive chemotherapy before operation, and all specimens were preserved at -80 °C. Before operation, all patients with cholangiocarcinoma were confirmed by pathological examination, and signed informed consent forms. The clinical features of cholangiocarcinoma patients were listed in **Table 1**. All procedures were in accordance with the 1964 Helsinki declaration and its later amendments or comparable ethical standards. The study was approved by the Ethics Committee of the Second Hospital of Hebei Medical University (No. 2020-R594).

3.2. Cell Culture and Transfection

Human cholangiocarcinoma cells (HCCC-9810, HuCCT1, and RBE) and the normal epithelial cell line hiBEC (BeNa Culture Collection, China) were placed in an incubator containing 95% air and 5% CO_2 at 37 °C and then cultured in DMEM with 10% FBS (Sigma-Aldrich, St. Louis, MO, USA). 100-U.mL^{-1} penicillin (Baomanbio, China) and 100-μg.mL^{-1} streptomycin

Table 1. Clinical features of cholangiocarcinoma patients(n=71)

Clinical information		Number of Cases(n=71)
Age	<55years	49
	≥55 years	22
Gender	Male	41
	Female	30
TNM stages	Stage I/II	44
	Stage III/IV	27
Lymph node metastasis	Yes	25
	No	46

Table 2. PCR primer sequences

Gene	Primer sequence
miR-582	F: 5'- GCACACATTGAAGAGGACAGAC- 3'
	R: 5'-TATTGAAGGGGGTTCTGGTG- 3'
U6	F：5'-CTCGCTTCGGCAGCACA- 3'
	R：5'-AACGCTTCACGAATTTGCGT- 3'
LIS1	F：5'-CGTCTCTGGTCACCTGTGTAA - 3'
	R：5'-CTCATGGCTGTCCGTCGAT- 3'
GAPDH	F：5'-AATGGACAACTGGTCGTGGAC- 3'
	R：5'-CCCTCCAGGGGATCTGTTTG- 3'

(Baomanbio, China) were added as required. miR-582 mimic (5'-UAACUGGUUGAACAACUGAACCAA-3'), mimic control (5'-UCACAACCUCCUAGAAAGAGUAGA-3'), miR-582-5p inhibitor (5′-AGUAACUGGUUGAACAACUGUAA-3′), and NC inhibitor (5′-CAGUACUUUUGUGUAGUACAAA-3′) were synthesized and purified by Shanghai GenePharma Co., Ltd. For cell transfection, HCCC-9810 and RBE cells were seeded into 6-well plates (5×10^5 cells/well) until reached 70%-90% confluency. When reaching, the cells were transfected following the instruction of Lipofectamine™ 2000 Reagent (Thermo Fisher, USA).

3.3. ART-PCR Analysis

Total RNAs were extracted from tissue samples by using TRIzol reagent (Invitrogen, Carlsbad, USA), and then were reverse transcribed into cDNA with First Strand cDNA Synthesis Kit (Sigma-Aldrich). TaqMan microRNA Assay Kit was used to analyze miR-582 and U6 expression. SYBR Green Gene Expression Assay Kit (QIAGEN) was used to detect LIS1 and GAPDH expression. A quantitative real-time PCR assay was performed on the ABI7500 Instrument (Applied Biosystems, Warrington, UK). Reaction conditions included: 95 °C for 30 s; 40 cycles of 95 °C for 5 s and 60 °C for 30 s. The primer sequences were listed as follows (**Table 2**). The experiments were repeated at least three times. Results were analyzed by $2^{-\Delta\Delta CT}$ method.

3.4. Dual Fluorescence Reporter Assay

TargetScan (http://www.targetscan.org) was used to predict the potential binding site of miR-582. Constructing pMIR-*LIS1*-Wt and pMIR-*LIS1*-Mut, HCCC-9810 cells were co-transfected with miR-NC, miR-582 mimics, NC-inhibitor or miR-582 inhibitor. After 24h of transfection, 100 μL cell lysates were added to each well. Then, cell lysate (20 μL/well) was added into a 96-well plate, and the luciferase activity was detected using a dual luciferase assay kit (Invitrogen, Thermo, USA). The ratio of firefly luciferase activity to sea kidney luciferase activity was regarded as the relative luciferase activity. Sequence was listed as below:

LIS1 3'UTR-WT

F：AAACTCGAGTTGTGTCTCCTTCGGCCC

F：AAAGCGGCCGCGGCATTTAATAGTTTACCAGTTGGT

LIS1 3'UTR-MUT

F：GTGAATCCAAATTGTATACTGTAAATTTACATACGTTGTCTAGA

R：TCTAGACAACGTATGTAAATTTAGACCCTACAATTTGGATTCAC

3.5. Western Blot

The cells or tissues were lysed employing RIPA lysis buffer (50 mMTris-HCl (pH 7.4), 150 mM NaCl, 1% NP-40, 0.1% SDS), and its concentration was measured by BCA method (Solarbio, R0010, China). 30-μg protein was added into SDS-PAGE(Solarbio, D1010, China) for gel electrophoresis, and then wet transferred to PVDF membrane (Zeye Bio Co., Ltd, China), sealed with 5% skim milk(Sangon Biotech, A600669, China) for 2h, and rinsed 3 times in TBST buffer(10 min/times); The *LIS1* antibody (1:500, Proteintech, 10592-1-AP, China), MMP-

2 antibody (1:500, Proteintech, 12171-1-AP, China), p-AKT antibody (1:500, Proteintech, 14026-1-AP, China), AKT antibody (1:500, Solarbio, SE131, China) and GAPDH antibody (1:1000, Proteintech, 60004-1-Ig, China)were added to the PVDF membrane and incubated overnight at 4 °C. Then they were supplemented by horseradish peroxidase labeled secondary antibody (1:1000, Solarbio, SE132, China), and incubated at room temperature for 1h. The protein expression level was detected using ECL chemiluminescence (Solarbio, PE0010, China) agent in dark room.

3.6. Fluorescence in Situ Hybridization

Isolated tissue was cut into tissue blocks ($1cm^2$x0.5cm), which were routinely fixed in 10% formaldehyde (YM-MY804J, Yuanmu, Shanghai, China) and paraffin-embedded. Each block was serially sectioned and stored at 4 °C for subsequent in situ hybridization. RNase contamination should be avoided during the whole process. FISH was used to detect the miR-582 expression in cholangiocarcinoma tissues and adjacent normal tissues. MiR-582 locked nucleic acid probe and miRNA ISH Optimization Kit (Exiqon, Denmark) were used to conduct ISH. Fluorescence microscope (Olympus, Japan) was used to examine the signal.

3.7. Immunohistochemistry

Paraffin sections were de-waxed and re-hydrated, followed by adding 3% H_2O_2 solution (10011218, Sinopharm, China) to incubate 15min at room temperature to block endogenous peroxidase activity. Sections were placed in citrate buffer, and microwave was used to repair antigen. 5% normal goat serum (SL038, Solarbio, China) was added for 15min blocking at room temperature. *LIS1* antibodies, Ki67 antibodies (27309-1-AP, Proteintech, China) or CK-19 antibodies (1:100, ThermoFisher, USA) were added to maintain overnight at 4 °C. Horseradish peroxidase labeled rabbit secondary antibody (1:200, A0277, Beyotime, China) was added for 30min incubation at 37 °C. Horseradish enzyme labeled streptavidin working solution (A0303, Beyotime, China) was dripped for 30 min incubation at 37 °C. After DAB color development (ab64238, Abcam, UK), hematoxylinwas was used to stain sections at room temperature.

3.8. CCK8 Assay

HCCC-9810 and RBE cells in logarithmic growth phase were digested with pancreatin (C0203, Beyotime, China) to obtain single cell suspension. Cells were inoculated into a 96-well plate (Thermo Fisher, USA) according to 200-μL cell suspension per well. After transfecting of 72 hours, the cells were incubated 1h at 37 °C after adding 10-μL CCK-8 solution (KGA3017, KeyGEN, China) in each well according to CCK-8 kit instruction. The value was detected at the 450nm wavelength using a microplate reader (ELX-800, USA, Bioteck).

3.9. Flow Cytometry Assay

HCCC-9810 and RBE cells were digested with 0.01% trypsin (C0203, Beyotime, China) for 30min, re-suspended with cold PBS (P10033, Double-helix, Shanghai, China), fixed in pre-cool 70% ethanol and maintained at 4 °C overnight. Removing the ethanol, the suspension was rinsed twice in PBS (P10033, Double-helix, Shanghai, China). Adding 100-μL RNase A, cells were stained 30 min using 400-μL PI at 37 °C and kept away from light for 30 min at 4 °C. Flow cytometry was performed to detect the cell cycle.

3.10. Transwell Assay

HCCC-9810 and RBE cells were inoculated into the upper transwell chamber (3422, Corning, USA) with Matrigel gel (BD Biosciences, CA, USA) for invasion assay or without Matrigel gel for migration assay, and were cultured at 37 °C for 24h. Later, 600-μL culture medium containing 10% serum (31800-014, Gibo, USA) was added into the lower chamber. The chamber was rinsed in PBS (P10033, Double-helix, Shanghai, China) for 3 times, followed by 5min fixation in 95% ethanol. After staining 10min in 0.5% crystal violet (0528, Amresco, USA), the chamber was rinsed in PBS to remove excess staining solution of unbound cells. Removing the upper-layer cells with a cotton swab, lower-layer cells were observed under a microscope (IX53, Japan, OLYMPUS).

3.11. Xenograft Model of Nude Mice with Cholangiocarcinoma

24 BALB/c nude mice aged 5 weeks (13 males, 11 females, 14-17g) were randomly divided into NC group, miR-582 group, NC-inhibitor group and miR-58 inhibitor group (n=6/group). All mice were kept at 22 °C and had ad libitum access to water and food. Transfecting HCC-9810 cells, 0.2 mL single cell suspension (1×10^6cells/mL) was injected subcutaneously into

the left upper armpit of the mice. After inoculation, the max diameter (a) and min diameter (b) of tumor volume were measured using a vernal caliper (formula $V=1/2\times A\times B^2$) every 3 days. Three weeks later, all nude mice were sacrificed, and tumor was stripped, weighed, photographed, and fixed with formaldehyde. The whole process was approved by the Ethics Committee of the Second Hospital of Hebei Medical University.

3.12. Statistical Analysis

IBM SPSS Statistics V22.0 was adopted to perform statistical analysis, and data were expressed as the mean±SD. The data between two groups were analyzed by T test, while data of three or more groups were examined by one-way ANOVA. Each experiment was repeated at least three times. $P<0.05$.

4. Results

4.1. MiR-582 Expression in Cholangiocarcinoma and Its Target Gene

To analyze the impacts of miRNA on the prognosis of cholangiocarcinoma patients, we downloaded the database of miRNA expression level and clinical features from TCGA-CHOL (The Cancer Genome Atlas). Patients were divided into two groups according to 3/4 quartile method, and their survival rates were compared between high expression group and low expression group. We found that miR-582 expression in cholangiocarcinoma tissues was much lower than that in adjacent normal tissues (**Fig. 1A**(**a**)). Then, we conducted log-rank tests to plot Kaplan-Meier survival curves, finding there was statistical significance between miR-582 and overall survival rate ($P>0.05$) (**Fig. 1A**(**b**)). In this study, miR-582 expression level was detected by qRT-PCR, showing miR-582 expression was much lower in cholangiocarcinoma tissues as compared to healthy normal tissues (**Fig. 1B**). Similarly, miR-582 expression was decreased in multiple cholangiocarcinoma cell lines when compared with epithelial cells hiBEC (**Fig. 1C**). Carrying out fluorescence in situ hybridization(FISH), we found that the positive signal of miR-582 in cholangiocarcinoma tissues was significantly reduced as compared with normal tissues in 3 representative pairs of tissues (**Fig. 1D**). This analysis suggested that miR-582 may play an anti-cancer role in cholangiocarcinoma. To investigate the potential target gene of miR-582, we examined Targetscan database and identified *LIS1* as a potential target for miR-582 (**Fig. 1E**). Dual luciferase reporter assay was performed to confirm whether *LIS1* was the target gene of miR-582. The results showed that luciferase activity was decreased when miR-582 mimics and pMIR-*LIS1*-wt plasmid were co-transfected into HCC-9810 cells, but it had no changes after co-transfecting miR-582 mimics and pMIR-*LIS1*-Mut plasmid into HCC-9810 cells (**Fig. 1F**). Moreover, transfection with miR-582 inhibitor led to a clear rise in the luciferase activity of pMIR-*LIS1*-wt plasmid, but no effects were observed on the luciferase activity of pMIR-*LIS1*-Mut plasmid (**Fig. 1F**). These identified the specific binding relation between miR-582 and 3′-UTR of *LIS1*.

4.2. MiR-582 Negatively Regulates LIS1 Expression

qRT-PCR indicated that miR-582 expression was increased, and *LIS1* mRNA level was reduced in miR-582 group as compared with NC group (**Fig. 1G, H**). Meanwhile, miR-582 expression was decreased, while mRNA expression of *LIS1* was increased in miR-582 inhibitor group (**Fig. 1G, H**). Western blotting was used to detect effects of miR-582 on *LIS1* expression, which showed miR-582 mimics could downregulate *LIS1* expression (**Fig. 1I**(**a**)), while transfection with miR-582 inhibitor produced an opposite effect (**Fig. 1I**(**b**)). These results indicated that miR-582 could negatively regulate its target gene *LIS1*.

4.3. LIS1 Expression in Cholangiocarcinoma

TCGA database revealed that *LIS1* was over-expressed in tumor samples compared with normal samples (**Fig. 2A**). However, the survival curve showed that *LIS1* had no significant correlation with patients' prognosis ($P>0.05$) (**Fig. 2B**). Detected by immunohistochemistry and Western blotting, the results showed that LIS1 was not overexpressed in the epithelial cells. (The positive staining of CK-19 and LIS1 not overlap). Immunohistochemistry showed that *LIS1* expression was higher in 4 representative pairs of cholangiocarcinoma tissue than in adjacent normal tissue (**Fig. 2C**). Western blotting revealed that *LIS1* expression was significantly higher in 1 representative pair of cholangiocarcinoma tissue than in adjacent normal tissue (**Fig. 2D**). qRT-PCR results showed that the mRNA expression of *LIS1* was increased in cholangiocarcinoma tissues as compared with adjacent normal tissues (**Fig. 2E**), suggesting a close relation between *LIS1* expression and cholangiocarcinoma.

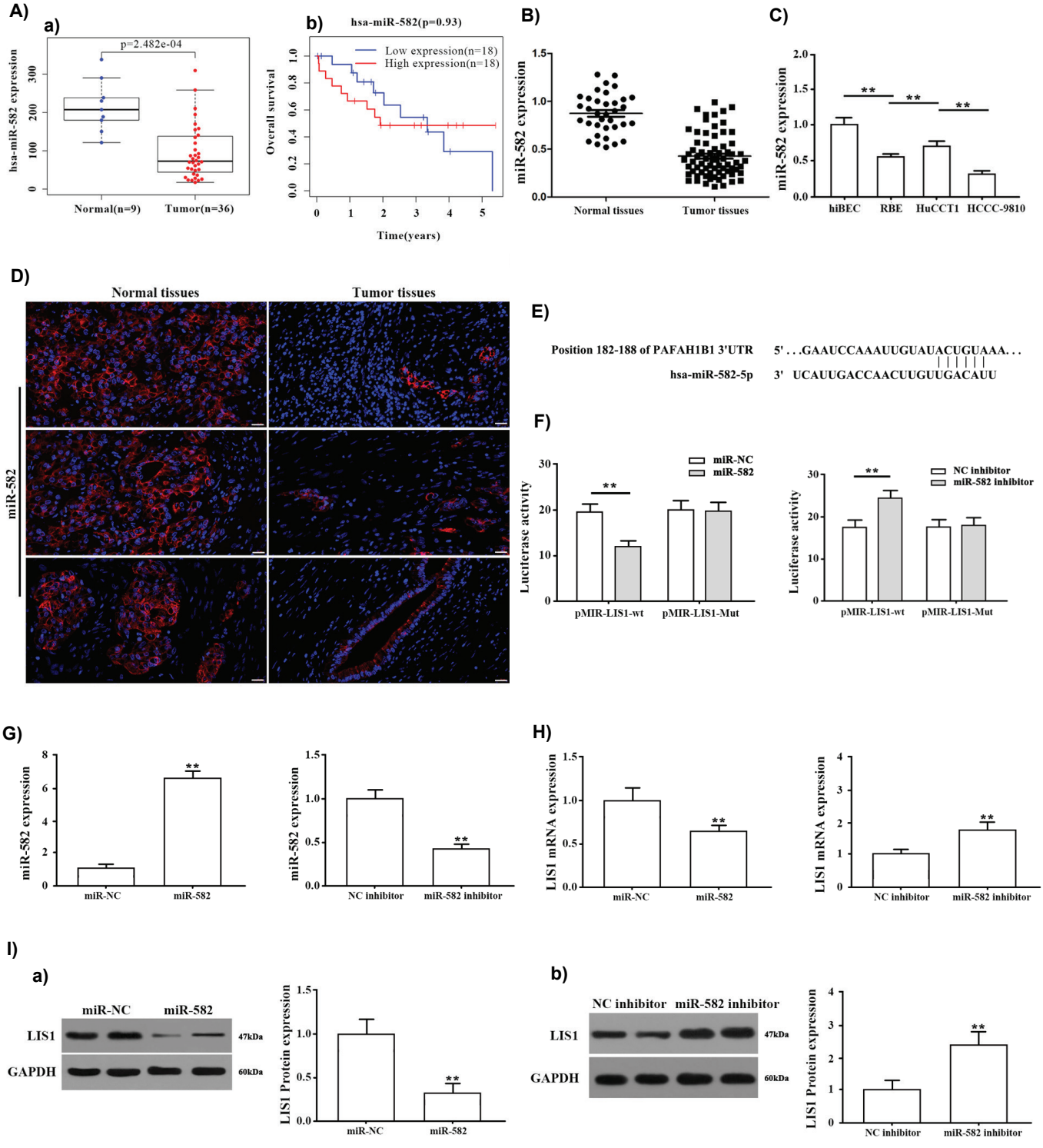

Figure 1. MiR-582 expression in cholangiocarcinoma: **A)** (**a**) miR-582 expression of cholangiocarcinoma samples from TCGA-CHOL database, (**b**) Survival curve of miR-582, **B)** qRT-PCR analyzed miR-582 expression in 71 cholangiocarcinoma tissues and 35 healthy tissues, **C)** qRT-PCR analyzed miR-582 expression in cell lines, **D)** FISH detected positive signal of miR-582(n=3), **E)** TargetScan predicted binding site of miR-582 on *LIS1* 3'-UTR, **F)** Dual luciferase reporter detected luciferase activity, and MiR-582 negatively regulated *LIS1* expression: **G)** miR-582 expression was detected by qRT-PCR, **H)** qRT-PCR was used to detect mRNA expression of *LIS1* gene, **I)** *LIS1* expression was detected by western blotting. (Scale bar=20μm).**P<0.01.

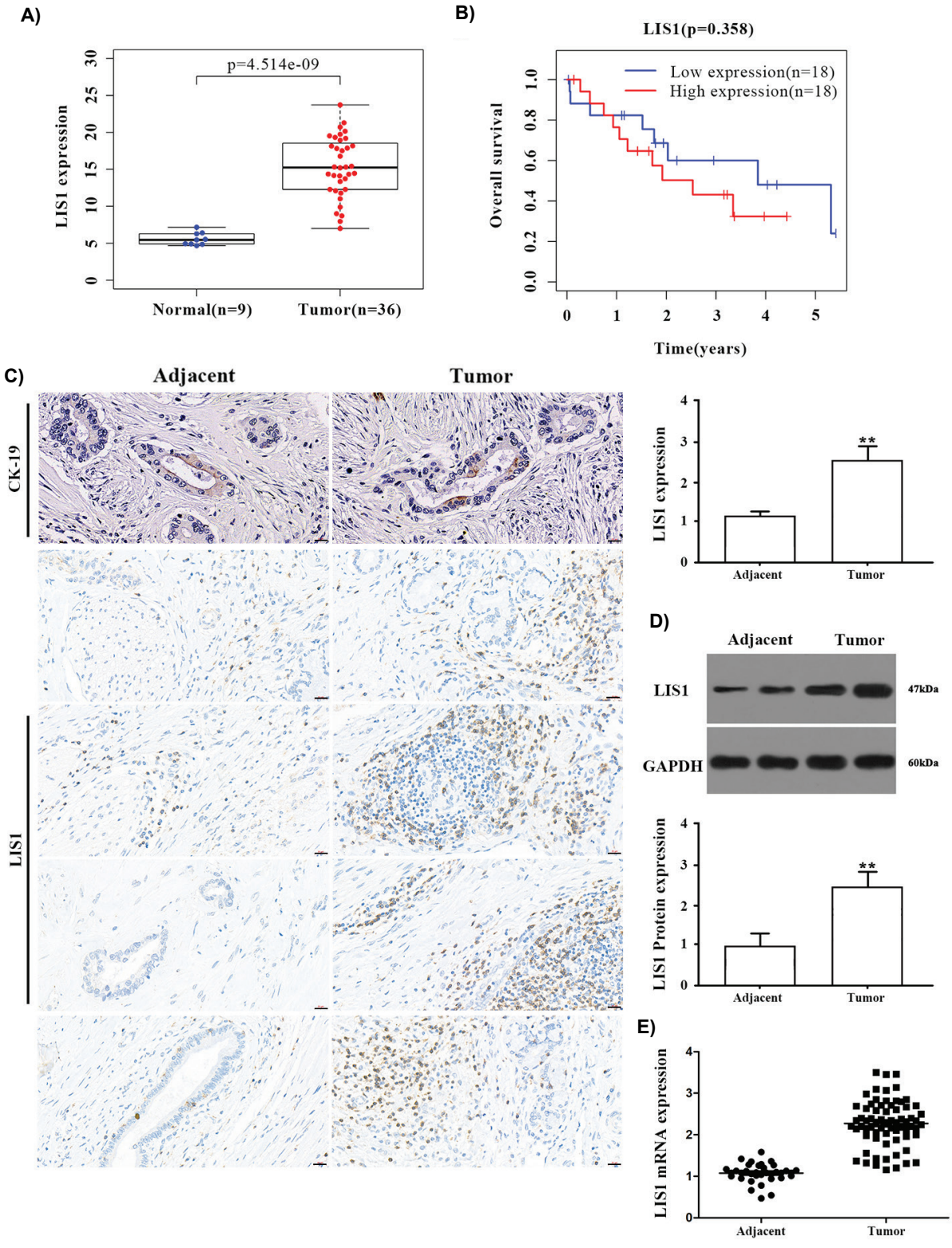

Figure 2. *LIS1* expression in cholangiocarcinoma. **A)** *LIS1* expression of cholangiocarcinoma samples from TCGA-CHOL database, **B)** Survival curve of *LIS1* in cholangiocarcinoma, **C)** Immunohistochemistry detected *LIS1* expression (n=4), **D)** Western blotting detected *LIS1* expression (n=1), **E)** qRT-PCR analyzed mRNA expression of LIS1 in 71 cholangiocarcinoma tissue samples and 35 healthy tissue samples.**P<0.01.

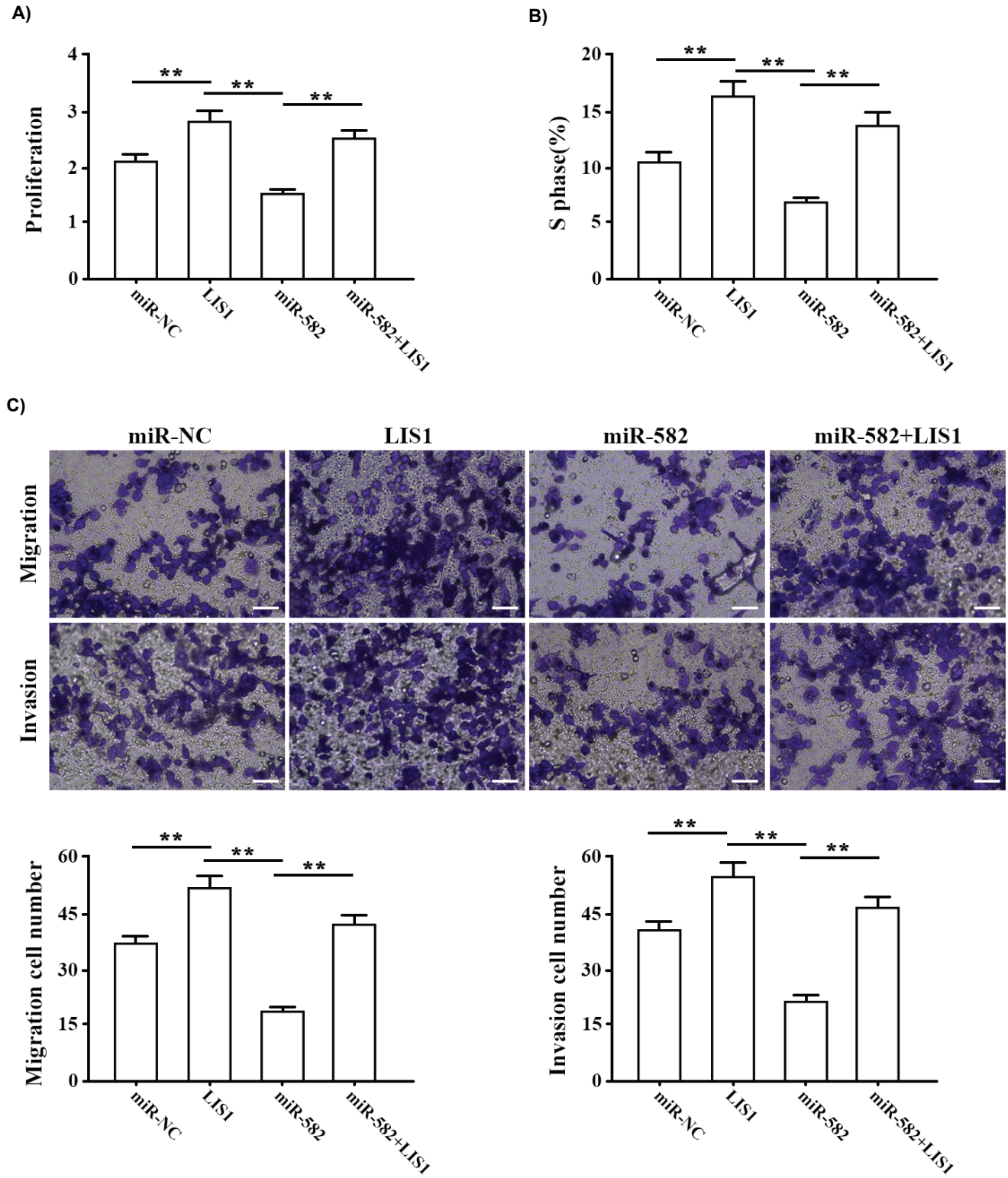

Figure 3. Effects of mir-582 mimics and *LIS1* on proliferation, cycle, migration and invasion of HCCC-9810 cells. **A)** Proliferation was detected by CCK8 assay, **B)** S-phase ratio was detected by flow cytometry assay, **C)** Migration and invasion were detected by Transwell assay. **P<0.01.

4.4. Effects of MiR-582 and LIS1 on Proliferation, Cell Cycle, Migration and Invasion of HCCC-9810 and RBE Cells

Influence of miR-582 mimics and *LIS1* on HCCC-9810 cell proliferation was detected by CCK8. The results showed that the proliferation of HCCC-9810 cells was clearly increased as compared with the NC group. *LIS1* was up-regulated, and miR-582 mimics was down-regulated. However, after co-transfection of miR-582 mimics and *LIS1,* miR-582 regulatory ability was reversed by *LIS1* (**Fig. 3A**). Then, S-phase ratio was detected by flow cytometry assay, showing *LIS1* overexpression could increase S-phase ratio, while up-regulation miR-582 inhibited S-phase arrest and such inhibition was counteracted by miR-582 and *LIS1* overexpression (**Fig. 3B**). Transwell assay was carried out to detect cell migration and invasion in each group, finding that the migration and invasion of cells with high *LIS1* expression were obviously larger than that in NC group.

Transfection of miR-582 mimics could inhibit migration and invasion, but *LIS1* could reverse such inhibition (**Fig. 3C**). Transfection of miR-582 inhibitor could promote proliferation, S-phase arrest, migration and invasion of HCCC-9810 cells, while transfection of *LIS1* siRNA could make it reverse **(Fig. 4A-C**). In addition, we repeated above experiments on RBE cells, and produced the same results (**Fig. S1 and Fig. S2**.). These results indicated that miR-582 is implicated in regulating the biological behavior of HCCC-9810 cells and RBE cells via negatively regulating *LIS1*.

4.5. Role of miR-582 in MMP-2 and p-AKT Expression

The expression of MMP-2 and p-AKT in HCCC-9810 cells transfected with miR-582 mimics or miR-582 inhibitor was detected by western blotting. Compared with NC group, the expression of MMP-2 and p-AKT was decreased in mice transfected with miR-582 mimics, but AKT expression remained unchanged (**Fig. 5A**). In addition, transfection of miR-582 inhibitor resulted in increased MMP-2 and p-AKT expression (**Fig. 5B**). Furthermore, *siLIS1* also decreased MMP-2 and p-AKT expression (**Fig. 5C**), suggesting that miR-582 could inhibit the expression of MMP-2 and p-AKT.

4.6. Role of miR-582 in Cholangiocarcinoma Xenograft Model of Nude Mice

MiR-582 mimics and miR-582 inhibitors were transfected into HCCC-9810 cells respectively, and then the cells were inoculated subcutaneously in nude mice to construct cholangiocarcinoma xenograft model. After 21 days, the tumor was stripped and weighed. It was found that the tumor volume and weight in miR-582 group were much lower than that in NC group, while the tumor volume in miR-582 inhibitor group was increased (**Fig. 6A, B**). Immunohistochemistry assay showed that Ki67 and *LIS1* expression of tumor tissues were lower in miR-582 group as comparing with NC group, while the higher level of Ki67 and *LIS1* expression was found in miR-582 inhibitor group (**Fig. 6C**). Western blotting showed that up-regulation of miR-582 could inhibit *LIS1* expression in tumor tissues (**Fig. 6D**), and downregulation of miR-582 produced the opposite effect (**Fig. 6E**).

5. Discussion

Cholangiocarcinoma is a cancer that forms in the bile ducts (26-27). MiRNA acts as a key role in embryogenesis, metabolism, apoptosis and tumor micro-environment (28-30). Huang *et al*. found that miR-582-3p and miR-582-5p were positively correlated with advanced pathological characteristics and shorter bone metastasis-free survival in prostate cancer (31). In our study, we examined TCGA database and found that miR-582 was decreased in tumor samples compared with normal samples. The working mechanism of miR-582 in cholangiocarcinoma was also explored through cellular experiments and animal model, finding down-regulation of miR-582 expression could be closely related to cholangiocarcinoma.

MiRNAs mainly bind to the 3′UTR of target mRNAs through complementary base pairing to cause mRNA degradation or translation inhibition (32-33). In this study, TargetScan showed that miR-582 had a potential binding site on 3’-UTR of *LIS1*. The dual-luciferase assay revealed up-regulation of miR-582 could inhibit the luciferase activity of *LIS1* wild-type 3’-UTR reporter gene plasmid, but down-regulation of miR-582 posed an opposite result. However, both up-regulation and down-regulation posed no obvious effects on luciferase activity of mutant reporter gene plasmid, indicating miR-582 can specifically bind to the 3’-UTR of *LIS1*. Furthermore, transfecting miR-582 mimics into HCCC-9810 cells could reduce mRNA and protein expression of *LIS1*, while transfection of miR-582 inhibitor could up-regulate *LIS1* expression.

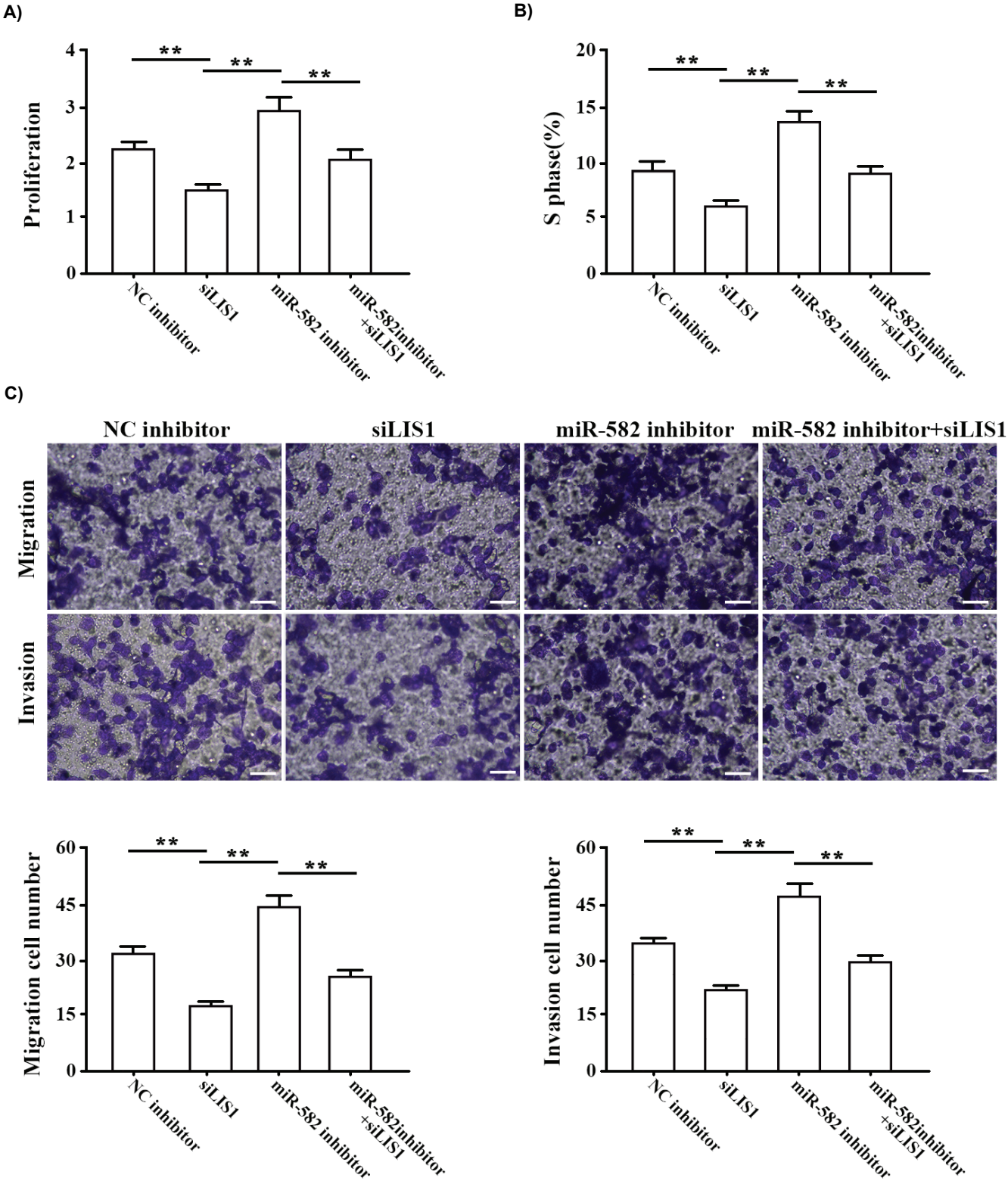

Figure 4. Effects of miR-582 inhibitor and *LIS1* on proliferation, cycle, migration and invasion of HCCC-9810 cells. **A)** Proliferation was detected by CCK8 assay, **B)** S-phase ratio was detected by flow cytometry assay, **C)** Migration and invasion were detected by Transwell assay. **P<0.01.

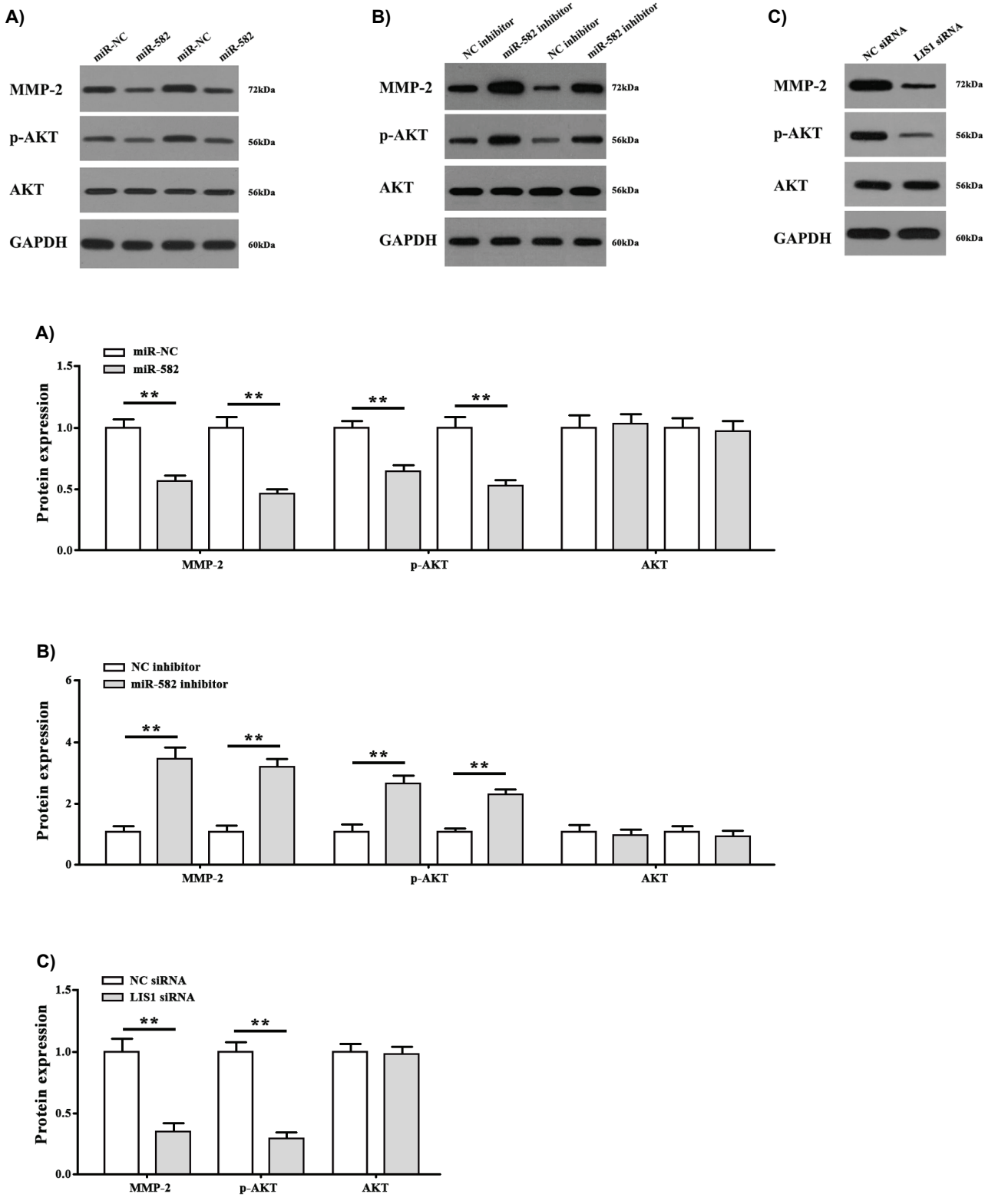

Figure 5. A) MMP-2, P-Akt and AKT expression was detected by Western blotting after transfecting miR-582 mimics, **B)** MMP-2, P-Akt and AKT was detected by Western blotting after transfecting miR-582 inhibitor, **C)** MMP-2, P-Akt and AKT was detected by Western blotting after adding *LIS1* siRNA. Experiment was repeated at least three times.

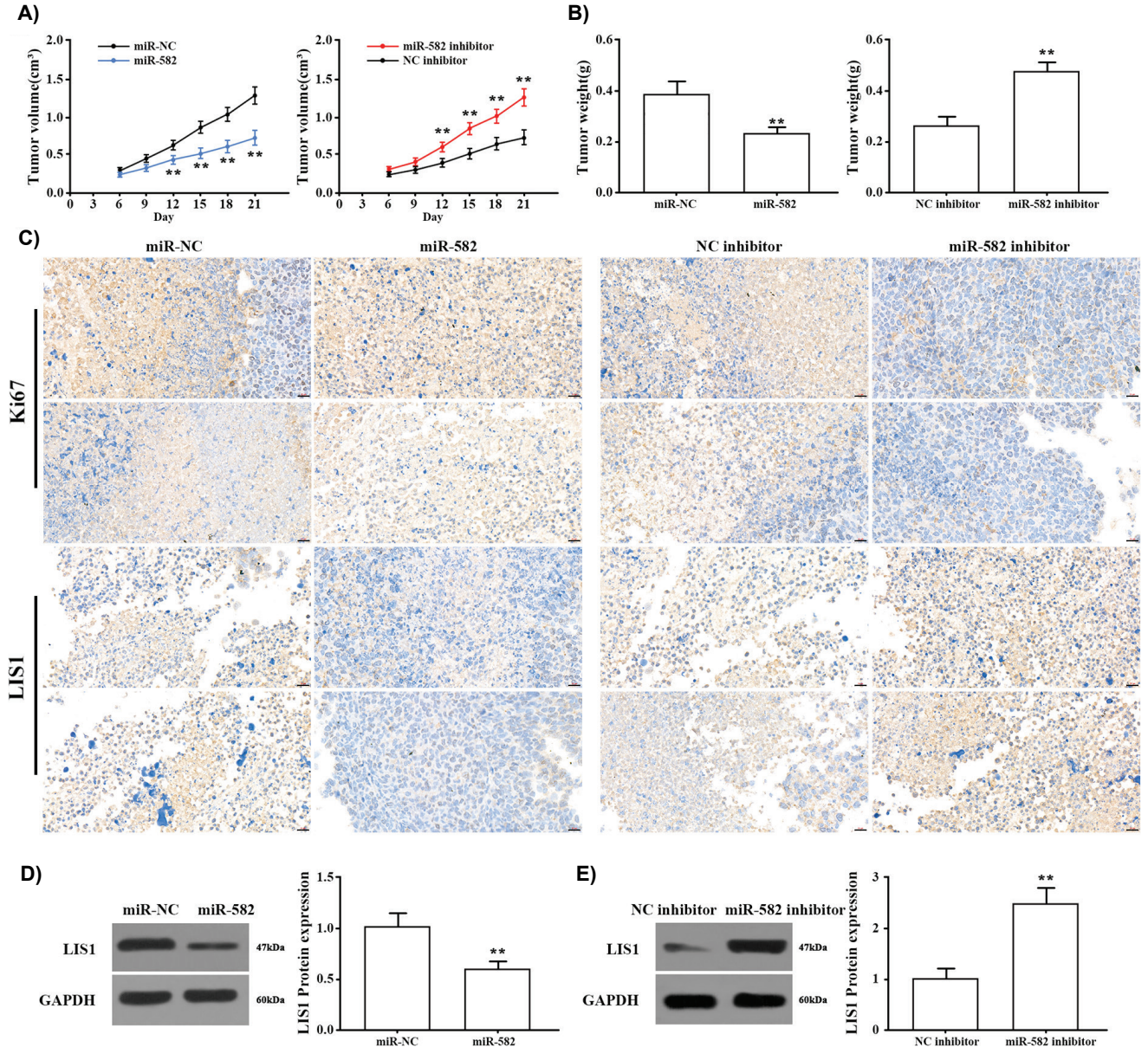

Figure 6. The role of miR-582 in cholangiocarcinoma xenograft model of nude mice. **A)** Tumor volume, **B)** Tumor weight, **C)** Immunohistochemistrywas was used to detect Ki67 and *LIS1* expression in tumor tissue, (**D&E**) *LIS1* expression was detected by western blotting.**P<0.01.

The results suggested that *LIS1,* as the target gene of miR-582, was negatively regulated by it.

Lissencephaly1 (*LIS1*) provides instructions for making a protein that is one sub-unit of PAFAH1B (platelet-activating factor acetyl hydrolase 1b), regulating cellular proliferation, migration in tumor development (34). Lo FY found that increasing *LIS1* protein can promote lung cancer cell migration and invasion (35). In this study, we found that mRNA and protein expression of *LIS1* was increased in tumor tissues, suggesting a close relation between abnormal *LIS1* expression and cholangiocarcinoma. Further experiments were repeated using HCC-9810 cells transfected with miR-582 mimics, and up-regulating *LIS1* expression promoted the biological behavior of cells and reversed the regulation of miR-582 mimics. Besides, down-

regulation of *LIS1* inhibited the biological behavior, whereas transfection of miR-582 inhibitor was on the flip side and could be offset by si*LIS1*.

In vitro experiments showed that miR-582 inhibited the biological behavior of cholangiocarcinoma cells by negatively regulating *LIS1*.

Abnormal activation of p-AKT causes tumor cell proliferation, angiogenesis and invasion via downstream signaling pathways (36-37). MMP-2, a member of matrix metalloproteinase family, plays a vital role in many pathological processes including tissue remodeling, inflammation and tumorigenesis (38). MMP-2 could stimulate the release of growth factors to facilitate tumor cell growth (39). MiR-582-3p regulates EG-VEGF-induced trophoblast invasion via repressing MMP-2 and MMP-9 (40). This study revealed up-regulation of miR-582 could inhibit the expression of MMP-2 and p-AKT, while transfection of miR-582 inhibitor could increase the expression, suggesting that miR-582 was likely involved in regulating cholangiocarcinoma cells via targeting *LIS1*. Then, establishing nude mice model of cholangiocarcinoma, we found that *LIS1* expression was decreased and the tumor growth was suppressed in miR-582-overexpressed nude mice, while down-regulation produced an opposite result. MiR-582 could pose anti-cancer effects on cholangiocarcinoma. However, miR-582 has hundreds of target genes, whether other targets could potentially interact with MMP-2 and other transcription factors, receptors, or signaling proteins that may regulate cell migration, invasion and proliferation will be a key point in our further research.

6. Conclusion

To sum up, miR-582 is dysregulated in cholangiocarcinoma. Up-regulation of miR-582 could reduce MMP-2 and p-AKT expression via *LIS1* to inhibit cholangiocarcinoma cell proliferation, S-phase arrest, migration and invasion, indicating miR-582 could exert inhibitory effects on cholangiocarcinoma.

Funding: This research was supported by the Medical Science Research Project of Hebei Province in 2021 (No.20210960).

Declarations of interest: none.

Data availability

The data and materials in the current study are available from the corresponding author on reasonable request.

Author contributions

GL and YZ conceived and designed the project. GL, TL, LM and JW acquired the data. GL, TL and YZ analyzed and interpreted the data. GL and YZ wrote the paper. All authors read and approved the manuscript.

References

1. Akita M, Hong SM, Sung YN, Kim M, Ajiki T, Fukumoto T, *et al.* Biliary intraductal tubule-forming neoplasm: a whole exome sequencing study of MUC5AC-positive and -negative cases. *Histopathology*. 2020;**76**(7):1005-1012. doi: 10.1111/his.14103.
2. Choodetwattana P, Proungvitaya S, Jearanaikoon P, Limpaiboon T. The Upregulation of OCT4 in Acidic Extracellular pH is Associated with Gemcitabine Resistance in Cholangiocarcinoma Cell Lines. *Asian Pac J Cancer Prev.* 2019;**20**(9): 2745-2748. doi: 10.31557/APJCP.2019.20.9.2745.
3. Cubero FJ, Mohamed MR, Woitok MM, Zhao G, Hatting M, Nevzorova Y, *et al*. Loss of c-Jun N-terminal Kinase 1 and 2 Function in Liver Epithelial Cells Triggers Biliary Hyperproliferation Resembling Cholangiocarcinoma. *Hepatol Commun*. 2020;**4**(6): 834-851. doi: 10.1002/hep4.1495.
4. Mcgrath NA, Fu J, Gu SZ, Xie C. Targeting cancer stem cells in cholangiocarcinoma (Review). *Int J Oncol*. 2020;**57**(2): 397-408. doi: 10.3892/ijo.2020.5074.
5. Phoomak C, Silsirivanit A, Park D, Sawanyawisuth K, Vaeteewoottacharn K, Wongkham C, *et al.* O-GlcNAcylation mediates metastasis of cholangiocarcinoma through FOXO3 and MAN1A1. *Oncogene*. 2018;**37**(42): 5648-5665. doi: 10.1038/s41388-018-0366-1.
6. Andrés-León E, Gómez-López G, Pisano DG. Prediction of miRNA-mRNA Interactions Using miRGate. *Methods Mol Biol*. 2017;**1580**: 225-237. doi: 10.1007/978-1-4939-6866-4_15.
7. Pieczora L, Stracke L, Vorgerd M, Hahn S, Theis V. Unveiling of miRNA Expression Patterns in Purkinje Cells During Development. *Cerebellum*. 2016;**16**(2): 1-12. doi: 10.1007/s12311-016-0814-9.
8. Yu X, Zhang L, Wen G, Zhao H, Luong L, Chen Q, *et al*. Upregulated sirtuin 1 by miRNA-34a is required for smooth muscle cell differentiation from pluripotent stem cells. *Cell Death Differ*. 2015;**22**(7):1170-1180. doi: 10.1038/cdd.2014.206.
9. Liu YL, Wang GQ, Cui HX, Li XX, Xu ZL, Wang XY. miRNA211 induces apoptosis of cervical cancer SiHa cells via down-regulation of inhibitor of apoptosis proteins. *Eur Rev Med Pharmacol Sci*. 2018; **22**(2):336-342. doi: 10.26355/eurrev_201801_14177.
10. Irani S, Hussain MM. Role of microRNA-30c in lipid metabolism, adipogenesis, cardiac remodeling and cancer. *Curr Opin Lipidol*. 2015;**26**(2):139-146. doi: 10.1097/MOL.0000000000000162.
11. Hartig SM, Hamilton MP, Bader DA, Mcguire SE. The miRNA Interactome in Metabolic Homeostasis. *Trends Endocrinol Metab*. 2015;**26**(12):733-745. doi: 10.1016/j.tem.2015.09.006.
12. Zheng B, Jeong S, Zhu Y, Chen L, Xia Q. miRNA and lncRNA as biomarkers in cholangiocarcinoma(CCA). *Oncotarget*. 2017;**8**(59):100819-100830. doi: 10.18632/oncotarget.19044.

13. Chu CH, Chou W, Wang F, Yeh CN, Chen TC, Yeh TS. Expression profile of microRNA-200 family in cholangiocarcinoma arising from choledochal cyst. *J Gastroenterol Hepatol*. 2016;**31**(5):1052-1059. doi: 10.1111/jgh.13204.
14. Shigehara K, Yokomuro S, Ishibashi O, Mizuguchi Y, Arima Y, Kawahigashi Y, *et al*. Real-time PCR-based analysis of the human bile microRNAome identifies miR-9 as a potential diagnostic biomarker for biliary tract cancer. *PLoS One*. 2011;**6**(8):e23584. doi: 10.1371/journal.pone.0023584.
15. Liu CH, Huang Q, Jin ZY, Xie F, Zhu C, Liu Z, *et al*. Circulating microRNA-21 as a prognostic, biological marker in cholangiocarcinoma. *J Cancer Res Ther*. 2018;**14**(1):220-225. doi: 10.4103/0973-1482.193125.
16. Deng G, Teng Y, Huang F, Nie W, Zhu L, Huang W, *et al*. MicroRNA-101 inhibits the migration and invasion of intrahepatic cholangiocarcinoma cells via direct suppression of vascular endothelial growth factor-C. *Mol Med Rep*. 2015;**12**(5):7079-7085. doi: 10.3892/mmr.2015.4239.
17. Atanasov G, Dietel C, Feldbrügge L, Benzing C, Krenzien F, Brandl A, *et al*. Angiogenic miRNAs, the angiopoietin axis and related TIE2-expressing monocytes affect outcomes in cholangiocarcinoma. *Oncotarget*. 2018;**9**(52):29921-29933. doi: 10.18632/oncotarget.25699.
18. Zhang H, Dai Q, Zheng L, Yuan X, Pan S, Deng J. Knockdown of circ_HIPK3 inhibits tumorigenesis of hepatocellular carcinoma via the miR-582-3p/DLX2 axis. *Biochem Biophys Res Commun*. 2020;**533**(3):501-509. doi: 10.1016/j.bbrc.2020.09.050.
19. Xu J, Zhang Y, Huang Y, Dong X, Xiang Z, Zou J, *et al.* circEYA1 Functions as a Sponge of miR-582-3p to Suppress Cervical Adenocarcinoma Tumorigenesis via Upregulating CXCL14. *Mol Ther Nucleic Acids*.2020;**22**:1176-1190. doi: 10.1016/j.omtn.2020.10.026.
20. Ye CY, Zheng CP, Zhou WJ, Weng SS. MiR-582-5p inhibits the growth and invasion of osteosarcoma cell by targeting NOVA1. *Eur Rev Med Pharmacol Sci*. 2020;**24**(21):11026-11031. doi: 10.26355/eurrev_202011_23587.
21. Jheng GW, Hur SS, Chang CM, Wu CC, Cheng JS, Lee HH, *et al. Lis1* dysfunction leads to traction force reduction and cytoskeletal disorganization during cell migration. *Biochem Biophys Res Commun*. 2018;**497**(3):869-875. doi: 10.1016/j.bbrc.2018.02.151.
22. Voigt A, Zintl F. Effects of retinoic acid on proliferation, apoptosis, cytotoxicity, migration, and invasion of neuroblastoma cells. *Med Pediatr Oncol*. 2003;**40**(4):205-213. doi: 10.1002/mpo.10250.
23. Kodani A, Kenny C, Lai A, Gonzalez D, Stronge E, Sejourne G, *et al*. Posterior Neocortex-Specific Regulation of Neuronal Migration by CEP85L Identifies Maternal Centriole-Dependent Activation of CDK5. *Neuron*. 2020;**106**(2):246-255.e6. doi: 10.1016/j.neuron.2020.01.030.
24. Brehar FM, Gafencu AV, Trusca VG, Fuior E, Arsene D, Amaireh M, *et al*. Preferential Association of Lissencephaly-1 Gene Expression with CD133+ Glioblastoma Cells. *J Cancer*. 2017;**8**(7):1284-1291. doi:10.7150/jca.17635.
25. Gao L, Xue B, Xiang B, Liu KJ. Arsenic trioxide disturbs the LIS1/NDEL1/dynein microtubule dynamic complex by disrupting the CLIP170 zinc finger in head and neck cancer. *Toxicol Appl Pharmacol*. 2020;**403**:115158. doi: 10.1016/j.taap.2020.115158.
26. Hsiao CY, Yang PC, Li X, Huang KW. Clinical impact of irreversible electroporation ablation for unresectable hilar cholangiocarcinoma. *Sci Rep*. 2020;**10**(1):10883. doi: 10.1038/s41598-020-67772-2.
27. Lv Y, Wang Z, Zhao K, Zhang G, Huang S, Zhao Y. Role of noncoding RNAs in cholangiocarcinoma (Review). *Int J Oncol*. 2020;**57**(1):7-20. doi: 10.3892/ijo.2020.5047.
28. Zhang JW, Wang X, Li GC, Wang D, Han S, Zhang Y, *et al.* MiR-30a-5p promotes cholangiocarcinoma cell proliferation through targeting SOCS3. *J Cancer*. 2020;**11**(12):3604-3614. doi: 10.7150/jca.41437.
29. Ihle MA, Trautmann M, Kuenstlinger H, Huss S, Heydt C, Fassunke J, *et al*. miRNA-221 and miRNA-222 induce apoptosis via the KIT/AKT signalling pathway in gastrointestinal stromal tumours. *Mol Oncol.* 2015;**9**(7):1421-1433. doi: 10.1016/j.molonc.2015.03.013.
30. Suzuki HI, Katsura A, Matsuyama H, Miyazono K. MicroRNA regulons in tumor microenvironment. *Oncogene*. 2015;**34**(24):3085-3094. doi: 10.1038/onc.2014.254.
31. Huang S, Zou C, Tang Y, Wa Q, Peng X, Chen X, *et al.* miR-582-3p and miR-582-5p Suppress Prostate Cancer Metastasis to Bone by Repressing TGF-β Signaling. *Mol Ther Nucleic Acids*.2019;**16**:91-104. doi:10.1016/j.omtn.2019.01.004.
32. Kwon H, Song K, Han C, Zhang J, Lu L, Chen W, *et al*. Epigenetic Silencing of miRNA-34a in Human Cholangiocarcinoma via EZH2 and DNA Methylation: Impact on Regulation of Notch Pathway. *Am J Pathol*. 2017;**187**(10):2288-2299. doi: 10.1016/j.ajpath.2017.06.014.
33. Xie Y, Wang Y, Li J, Hang Y, Jaramillo L, Wehrkamp C, *et al*. Cholangiocarcinoma therapy with nanoparticles that combine downregulation of MicroRNA-210 with inhibition of cancer cell invasiveness. *Theranostics*. 2018;**8**(16):4305-4320. doi: 10.7150/thno.26506.
34. Escamez T, Bahamonde O, Tabares-Seisdedos R, Vieta E, Martinez S, Echevarria D. Developmental dynamics of PAFAH1B subunits during mouse brain development. *J Comp Neurol*. 2012;**520**(17):3877-3894. doi: 10.1002/cne.23128.
35. Lo FY, Chang JW, Chang IS, Chen YJ, Hsu HS, Huang SK, *et al.* The database of chromosome imbalance regions and genes resided in lung cancer from Asian and Caucasian identified by array-comparative genomic hybridization. *BMC Cancer*.2012;**12**:235. doi: 10.1186/1471-2407-12-235.
36. Zhang Y, Lv J, Guo H, Wei X, Li W, Xu Z. Hypoxia-induced proliferation in mesenchymal stem cells and angiotensin II-mediated PI3K/AKT pathway. *Cell Biochem Funct*. 2015;**33**(2):51-58. doi:10.1002/cbf.3080.
37. Yin Q, Jiang D, Li L, Yang Y, Wu P, Luo Y, *et al.* LPS Promotes Vascular Smooth Muscle Cells Proliferation Through the TLR4/Rac1/Akt Signalling Pathway. *Cell Physiol Biochem*. 2017;**44**(6):2189-2200. doi:10.1159/000486024.
38. Ma C, Peng C, Lu X, Ding X, Zhang S, Zou X, *et al.* Downregulation of FOXP3 inhibits invasion and immune escape in cholangiocarcinoma. *Biochem Biophys Res Commun.* 2015;**458**(2):234-239. doi:10.1016/j.bbrc.2015.01.067.
39. Li Z, Takino T, Endo Y, Sato H. Activation of MMP-9 by membrane type-1 MMP/MMP-2 axis stimulates tumor metastasis. *Cancer Sci*. 2017;**108**(3):347-353. doi: 10.1111/cas.13134.
40. Su MT, Tsai PY, Tsai HL, Chen YC, Kuo PL. miR-346 and miR-582-3p-regulated EG-VEGF expression and trophoblast invasion via matrix metalloproteinases 2 and 9. *Biofactors*. 2017;**43**(2):210-219. doi:10.1002/biof.1325.